at least several hundreds of AGN deg^{-2} with $z > 1$ and $\log L_X > 44$, assuming a 4:1 ratio of obscured to unobscured sources. Although this estimation falls well short of the current 850-μm source counts (8000 ± 3000 deg^{-2} at 1 mJy) (*30*), the AGN x-ray luminosity function has a large uncertainty at $z > 2$, which is the epoch in which the majority of luminous submillimeter galaxies are found (*32*). Furthermore, the space density of obscured AGN at high redshift is unknown: the x-ray background intensity does not preclude the existence of a large population of high redshift, Compton-thick sources.

References and Notes

1. J. Kormendy, K. Gebhardt, in *The 20th Texas Symposium on Relativistic Astrophysics*, H. Martel, J. C. Wheeler, Eds. (American Institute of Physics, in press) (e-Print available at http://xxx.lanl.gov/abs/astro-ph/0105230).
2. M. Schönberg, S. Chandrasekhar, *Astrophys. J.* **96**, 161 (1942).
3. G. Hasinger, in *ISO Surveys of a Dusty Universe*, D. Lemke, M. Stickel, K. Wilke, Eds. (Springer, New York, in press) (e-Print available at http://xxx.lanl.gov/abs/astro-ph/0001360).
4. M. R. S. Hawkins, *Astron. Astrophys. Suppl.* **143**, 465 (2000).
5. M. J. Page, J. P. D. Mittaz, F. J. Carrera, *Mon. Not. R. Astron. Soc.* **325**, 575 (2001).
6. M. J. Page, K. O. Mason, I. M. McHardy, L. R. Jones, F. J. Carrera, *Mon. Not. R. Astron. Soc.* **291**, 324 (1997).
7. A. C. Fabian, K. Iwasawa, *Mon. Not. R. Astron. Soc.* **303**, L34 (1999).
8. R. Gilli, G. Risaliti, M. Salvati, *Astron. Astrophys.* **347**, 424 (1999).
9. P. Ciliegi *et al.*, *Mon. Not. R. Astron. Soc.* **277**, 1463 (1995).
10. Observations were carried out in photometry mode using a standard chop/nod/jiggle observing technique. The atmospheric transmission and "submillimeter seeing" were at all times in the top quartile of values measured on Mauna Kea ($\tau < 0.2$, seeing < 0.5 arcsec). STARLINK SURF software was used to correct for the nod, flatfield, extinction, and despike and to remove sky noise from the data. Flux calibration was made against the primary submillimeter calibrator, Mars.
11. W. S. Holland *et al.*, *Mon. Not. R. Astron. Soc.* **303**, 659 (1999).
12. A. E. Hornschemeier *et al.*, *Astrophys. J.* **554**, 742 (2001).
13. A. J. Barger, L. L. Cowie, R. F. Mushotzky, E. A. Richards, *Astron. J.*, **121**, 662 (2001) (e-Print available at http://xxx.lanl.gov/abs/astro-ph/0007175).
14. P. Severgnini *et al.*, *Astron. Astrophys.* **360**, 457 (2000).
15. A. C. Fabian *et al.*, *Mon. Not. R. Astron. Soc.* **315**, L8 (2000).
16. N. Gehrels, *Astrophys. J.* **303**, 336 (1986).
17. J. J. Condon *et al.*, *Astron. J.* **115**, 1693 (1998).
18. R. B. Rengelink *et al.*, *Astron. Astrophys. Suppl.* **124**, 259 (1997).
19. R. D. Hildebrand, *Q. J. R. Astron. Soc.* **24**, 267 (1983).
20. D. Rigopoulou, A. Lawrence, M. Rowan-Robinson, *Mon. Not. R. Astron. Soc.* **278**, 1049 (1996).
21. M. Rowan-Robinson, *Mon. Not. R. Astron. Soc.* **316**, 885 (2000).
22. R. Genzel *et al.*, *Astrophys. J.* **498**, 579 (1998).
23. D. Downes, P. M. Solomon, *Astrophys. J.* **507**, 615 (1998).
24. M. Elvis *et al.*, *Astrophys. J. Suppl.* **95**, 1 (1994).
25. If our objects are systematically underluminous in x-rays, then we would be underestimating the bolometric luminosities of their active nuclei. However, this is unlikely because these sources were found in an x-ray survey, in which the natural selection bias is expected to favor sources with higher-than-average x-ray to bolometric luminosity ratios rather than lower-than-average ones.
26. E. N. Archibald *et al.*, *Mon. Not. R. Astron. Soc.* **323**, 417 (2001).
27. L. A. Nolan *et al.*, *Mon. Not. R. Astron. Soc.* **323**, 308 (2001).
28. I. Smail, R. J. Ivison, A. W. Blain, *Astrophys. J.* **490**, L5 (1997).
29. R. J. Ivison *et al.*, *Mon. Not. R. Astron. Soc.* **315**, 209 (2000).
30. A. W. Blain, J.-P. Kneib, R. J. Ivison, I. Smail, *Astrophys. J.* **512**, L87 (1999).
31. T. Miyaji, G. Hasinger, M. Schmidt, *Astron. and Astrophys.* **369**, 49 (2001).
32. J. S. Dunlop, *N. Astron. Rev.* **45**, 609 (2001).
33. B. T. Draine, H. M. Lee, *Astrophys. J.* **285**, 89, (1984).

34. The JCMT is operated on behalf of the Particle Physics and Astronomy Research Council of the United Kingdom, the Netherlands Organization for Scientific Research, and the National Research Council of Canada.

31 August 2001; accepted 16 October 2001
Published online 1 November 2001;
10.1126/science.1065880
Include this information when citing this paper.

Fermi Surface Sheet–Dependent Superconductivity in 2*H*-$NbSe_2$

T. Yokoya,[1]* T. Kiss,[1] A. Chainani,[1,2] S. Shin,[1,3] M. Nohara,[4] H. Takagi[4]

High-resolution angle-resolved photoemission spectroscopy was used to study the superconducting energy gap and changes in the spectral function across the superconducting transition in the quasi–two-dimensional superconductor 2*H*-$NbSe_2$. The momentum dependence of the superconducting gap was determined on different Fermi surface sheets. The results indicate Fermi surface sheet–dependent superconductivity in this low–transition temperature multiband system and provide a description consistent with thermodynamic measurements and the anomalous de Haas–van Alphen oscillations observed in the superconducting phase. The present data suggest the importance of Fermi surface sheet–dependent superconductivity in explaining exotic superconductivity in other multiband systems with complex Fermi surface topology, such as the borides and f-electron superconductors.

The energy gap in the single-particle excitation spectrum of the superconducting state makes the superconducting properties of a material qualitatively different from its normal-state properties. BCS (Bardeen, Cooper, and Schrieffer) theory (*1*) assumes electron-electron pairing to be due to phonons and approximates the pairing strength as a function of momentum to be constant, leading to an isotropic s-wave gap. This is not the case for high–transition temperature superconductors (high-T_c's), where a highly anisotropic $d_{x^2-y^2}$ gap has been confirmed (*2*, *3*) and unconventional pairing mechanisms other than electron-phonon interaction are actively considered (*4*). On the other hand, even for phonon-mediated s-wave superconductors, the existence of several Fermi surface (FS) sheets possessing different electron-phonon coupling constants and/or differing density of states (DOS) at the Fermi level (E_F) can give rise to a momentum-dependent superconducting gap in real materials (*5*, *6*). However, although tunneling studies (*5*) have deduced a momentum-dependent gap from momentum-averaged spectra, there is no direct experimental evidence based on momentum-resolved spectra to substantiate that claim.

We show that the electronic structure of 2*H*-$NbSe_2$ (*7*), a quasi–two-dimensional incommensurate charge density wave (CDW) system ($T_{CDW} \sim 35$ K) that is also a phonon-mediated superconductor below $T_c = 7.2$ K, exhibits FS sheet–dependent superconductivity. The result highlights the importance of FS sheet dependence of electronic structure and electron-phonon interactions in low-T_c superconductors.

Angle-resolved photoemission spectroscopy (ARPES) allows determination of the energy and momentum distribution of occupied electrons in a solid. For a given energy of incident photons, the energy distribution curve (EDC) measured at a fixed momentum and, conversely, the momentum distribution curve (MDC) measured at a fixed energy, directly represent the nature of the electronic states of a system. Thus, typically, ARPES can measure the Fermi momentum (k_F) as the point in momentum space corresponding to a band crossing E_F, with the locus of measured k_F's forming a Fermi surface. At a selected momentum vector on a FS, a temperature-dependent ARPES study can also measure the opening of a superconducting gap in the

[1]Institute for Solid State Physics, University of Tokyo, Kashiwa, Chiba 277-8581, Japan. [2]Institute for Plasma Research, Bhat, Gandhinagar-382 428, India. [3]The Institute of Physical and Chemical Research (RIKEN), Sayo-gun, Hyogo 679-5143, Japan. [4]Department of Advanced Materials Science, University of Tokyo, Tokyo 113-0033, Japan.

*To whom correspondence should be addressed. E-mail: yokoya@issp.u-tokyo.ac.jp

single-particle excitation spectrum across the superconducting T_c. In addition, ARPES has been used to extract the imaginary part of the self energy from EDC and MDC widths, which reflect the inverse lifetime and mean free path, respectively, for the suitable case of a single band crossing E_F at k_F (*8*–*10*).

The intensity map of the ARPES spectra from single-crystal 2*H*-$NbSe_2$ (0001), measured at $T = 10$ K with He IIα resonance line (Fig. 1A), obtained as a function of binding energy and momentum corresponds to the metallic phase exhibiting incommensurate CDW order. The direction in momentum space is along the blue line shown in Fig. 1C in which the two-dimensional Brillouin zone of 2*H*-$NbSe_2$ is depicted. Dispersive bands are seen as bright regions of the intensity map, on which peak positions of a second derivative intensity plot are superimposed with light blue lines (or broken lines for weaker structures). At high binding energies (0.5 to 6.0 eV), we observe eight bands, indicated by the overlaid lines in Fig. 1A dispersing symmetrically about the Γ point. The bands move toward or away from E_F, with a minimum or maximum in the binding energy as they disperse away from the Γ point. These observations enable a highly accurate determination of the Γ point in momentum space (± 0.02 Å^{-1}). This identification of the position of the Γ point in momentum space was central to identifying the complex FS discussed below. In addition, we observe an intense band structure near E_F. By comparison with the calculated band structure of 2*H*-$NbSe_2$ (*11*), the former bands and the latter intense structure are seen to have a dominant Se 4p and Nb 4d character, respectively.

Figure 1B shows an enlargement of the narrow region near E_F in Fig. 1A. A band approaches E_F as a function of momentum and loses considerable intensity at E_F, indicative of a band crossing. To characterize the band crossing, we constructed an MDC plot at E_F with an energy window of ± 10 meV for the EDCs (Fig. 1D). The MDC at E_F shows a peak and a shoulder, which correspond to the two-peak structure in the MDC at 50-meV binding energy. This two-peak structure indicates two-band crossings and agrees well with band-structure calculations that predict two Nb 4d–derived bands crossing along the measured direction (*11*). A previous study was unable to distinguish between these two-band crossings (*12*, *13*). We looked carefully for the small FS around the Γ point, which is also predicted by band-structure calculations and has been observed by de Haas–van Alphen (dHvA) measurements in the superconducting state (*11*, *14*). Figure 1E shows MDCs as a function of binding energy on an intensity scale that is 20 times that shown in Fig. 1D. The MDC at E_F has two broad features positioned symmetrically with respect to the Γ point, and each feature follows a systematic band dispersion to the higher energies, confirming the existence of the small, holelike FS centered at the Γ point. Because band-structure calculations (*11*) show that Nb 4d dominated large hexagonal FS sheets around Γ(A) and K(H) points in the Brillouin zone and a small, pancakelike Se 4p dominated FS sheet around the Γ point, the present findings resolve all of these FS sheets. Previous ARPES measurements have not been able to provide a detailed map of the FSs in this multiband system, although the hexagonal surface has been identified (*12*, *13*). From an extensive set of ARPES intensity maps, the experimental FS sheets thus obtained can be plotted (Fig. 1C).

The above measurements at T = 10 K provide a precise value of E_F crossings in momentum space above the superconducting transition and, thus, facilitate a study of the superconducting gaps as a function of momentum (*15*). To study the superconducting gap on different FS sheets, we obtained temperature-dependent spectra at momentum points on the dominantly Se 4p– and Nb 4d–derived sheets [arising from the 16th, 17th, and 18th bands as numbered in (*11*)] using He Iα resonance line with a resolution of 2.5 meV. The measured locations in momentum space are shown in each inset as red circles (*16*). For the dominantly Se 4p–derived band (Fig. 2A), the spectra measured at 10 K and 5.3 K, which is above and below $T_c = 7.2$ K, do not show a leading-edge shift or a superconducting coherent peak, indicating that the superconducting gap does not open, or is very small if it even exists. The spectra show changes derived from the temperature dependence of the Fermi distribution function with a gap of $\Delta = 0$ meV. Given the accuracy of our measurements and the step size of the measurement, we estimate an upper limit of the gap of 0.2 ± 0.1 meV. In contrast, the results obtained on the dominantly Nb 4d–derived FS (Fig. 2, B and C) show a shift of the leading edge corresponding to the opening of a superconducting gap with a coherent peak. This confirms the existence of a momentum-dependent superconducting gap as determined by ARPES in a system other than the high-T_c cuprates. The momentum-resolved superconducting gaps have been simulated with the BCS spectral function as described previously for the cuprates (*17*). The magnitude of the gaps are 1.0 ± 0.1 meV for the point on the 17th band (Fig. 2B) and 0.9 ± 0.1 meV for the point on the 18th band (Fig. 2C) (*18*), yielding gap values of 1.22 and 1.13 meV at T = 0 K, assuming that temperature dependence of the gap follows weak-coupling BCS or strong-coupling theory (*1*).

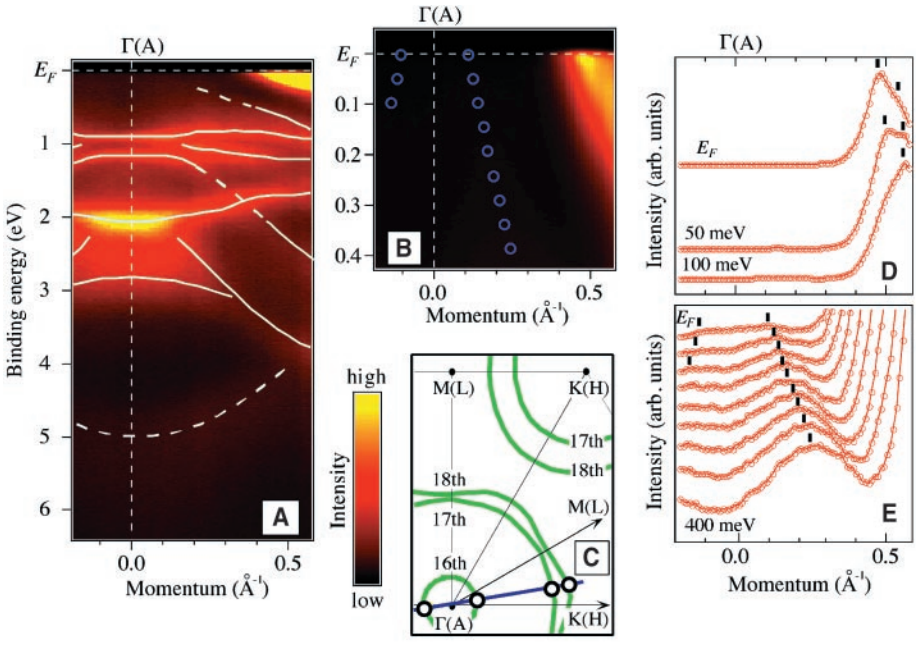

Fig. 1. (**A**) An intensity map of ARPES spectra for the entire valence-band region from single-crystal 2*H*-$NbSe_2$ (0001) measured at 10 K and (**B**) an enlargement of the region near E_F shown in (A). The EDCs were measured along the blue line in (**C**), which shows the experimentally obtained FS sheets (green curves). (**D** and **E**) MDCs at E_F and at values up to 100 meV (D) and 400 meV (E), plotted in steps of 50 meV, showing band dispersions for the dominantly Nb 4d–derived intense structures and the Se 4p–derived weak features close to the Γ point. The position of the Se 4p bands was confirmed to be symmetric in momentum space with respect to the Γ point [blue circles in (B)], although the measurement geometry results in unequal intensities for the weak features about the Γ point.

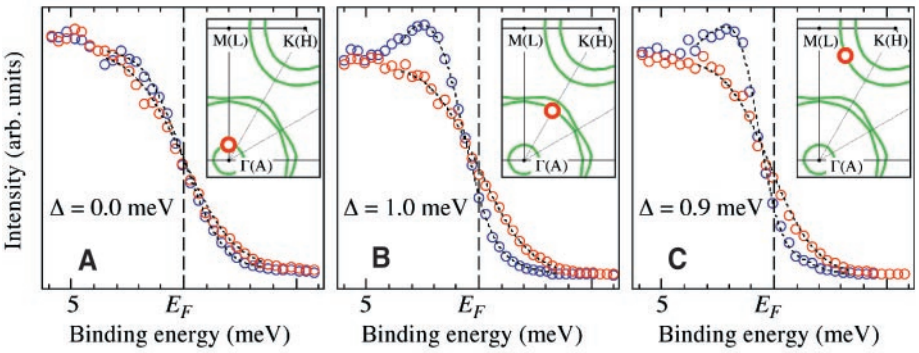

Fig. 2. (**A** to **C**) Temperature-dependent ultrahigh-resolution ARPES data, measured at FS sheets (red circles in each inset) arising from the Se 4p–derived 16th (A) and the Nb-derived 17th and 18th bands (B and C), as described in the band-structure calculations (*11*). The blue and red circles correspond to the measured ARPES spectra obtained at 5.3 K (superconducting state) and 10 K (normal state), respectively. We used high resolution (2.5 meV) and small step size (0.3 meV) to detect spectral changes as a function of temperature. The black dotted lines superimposed on the measured spectra are the numerical calculation results. The superconducting gap size Δ used for fitting the superconducting state spectrum is indicated in each panel.

The reduced gap value $2\Delta(0)/k_BT_c$ (where k_B is the Botzmann constant) is determined to be 3.6 to 3.9 for 2*H*-$NbSe_2$, indicating weak- to moderately strong-coupling superconductivity, and is consistent with the tunneling (*19*), Raman (*20*), and far-infrared transmission (*21*) measurements.

In contrast to the techniques that measure an average gap, the present results establish the existence of substantially different superconducting gap values on different FS sheets. Such a large difference in gap values on different FS sheets provides a simpler explanation for the results showing that the specific-heat γ values as a function of magnetic-field strength (*H*) in this compound (*22*) deviate from the linear dependence on *H* that is expected for conventional superconductors with a momentum-independent gap. The possibility of a smaller gap on the pancakelike sheet has been speculated from quantum oscillation signals in the mixed state of dHvA (*11*, *14*), although the origin of the effect is not yet fully understood. Corcoran *et al*. (*11*) deduced a gap value $\Delta(0) = 0.6$ meV and a low value of the electron-phonon coupling constant $\lambda = 0.3$ for this sheet, compared with the Nb-derived FS sheets. Further, the scanning tunneling spectroscopy study (*19*) carried out at 50 mK reported an s-wave–like gap with an average value of 1.1 meV and a variation of 0.7 to 1.4 meV. The lowest gap value of 0.7 meV is similar to that estimated from dHvA measurements. These measurements may be considered to be consistent with the present ARPES results, if the gap on the pancake surface opens up at a lower temperature. Because the measured temperature of 5.3 K is the lowest temperature we can attain, whether or not the gap on the pancake surface opens at a lower temperature will depend on further progress in refining the experimental technique.

According to BCS theory, the T_c of phonon-mediated superconductivity is given by $T_c = 1.13\ \theta_D \exp[-1/N(E_F)V]$, where θ_D is the Debye temperature, $N(E_F)$ is the DOS at E_F, and V is the average electron-pair interaction (*1*). Band-structure calculations indicate that the $N(E_F)$ derived from the Se dominant band is expected to be substantially smaller than that of the Nb dominant band. The dHvA measurements (*11*) reported a small value of $\lambda = 0.3$ for the dominantly Se-derived FS and estimated a large value for Nb-derived sheets by comparison with the specific-heat γ value. The smaller $N(E_F)$ and λ values, arising from differences in the Se 4p and Nb 4d electronic states and resulting differences in electron-phonon coupling, give rise to differences in the size of the superconducting gaps on different FS sheets.

The finding of a FS sheet–dependent superconducting gap shows the importance of a careful analysis of electronic structure as derived from the different character of electronic states and the resulting electron-phonon interactions in investigating the origin of superconductivity in low-T_c materials. The present results may provide insight into exotic superconductivity in other multiband systems with complicated FS topology, including f-electron superconductors (*23*) and borides (*24*).

References and Notes

1. J. R. Schrieffer, *Theory of Superconductivity* (Perseus Books, Reading, MA, 1983).
2. Z.-X. Shen *et al.*, *Phys. Rev. Lett.* **70**, 1553 (1993).
3. H. Ding *et al.*, *Phys. Rev. B* **54**, R9678 (1996).
4. P. W. Anderson, *The Theory of Superconductivity in the High-T_c Cuprates* (Princeton Univ. Press, Princeton, NJ, 1997).
5. G. Binnig, A. Baratoff, H. E. Hoenig, J. G. Bednorz, *Phys. Rev. Lett.* **45**, 1352 (1980).
6. T. Yokoya *et al.*, *Phys. Rev. Lett.* **85**, 4952 (2000).
7. The single crystals of 2*H*-$NbSe_2$ used in this study were prepared with an iodine-assisted chemical transport method (*22*). Magnetization and specific-heat measurements confirmed that the samples exhibit superconductivity below 7.2 K. ARPES measurements were performed on a spectrometer built with a Scienta SES2002 electron analyzer and a GAMMADATA high-flux discharging lamp with a toroidal grating monochromator. The energy and angular resolution determined with He IIα (40.814 eV) resonance lines were set to 14 meV and ± 0.1° (corresponding to 0.010 $Å^{-1}$), respectively. The He Iα (21.218 eV) measurements were set to a resolution of 2.5 meV and ± 0.1° (corresponding to 0.0067 $Å^{-1}$). Samples were cooled by using a flowing liquid He refrigerator with improved thermal shielding. Sample temperature was measured with a Si-diode sensor mounted below the samples. The base pressure of the spectrometer was $< 5 \times 10^{-11}$ Torr. The sample orientation was measured ex situ by using Laue photography and checked in situ by examining the symmetry of ARPES spectra. All measurements were done within 4 hours after in situ cleavings. Temperature-dependent spectral changes were confirmed by cycling temperature across T_c. E_F of samples for ultrahigh-resolution measurements at 2.5-meV resolution was referenced to that of a Au film evaporated onto the sample substrate, and its accuracy was estimated to be $< \pm 0.05$ meV from the difference in E_F before and after sample measurements.
8. T. Valla *et al.*, *Science* **285**, 2110 (1999).
9. M. R. Norman *et al. Phys. Rev. B* **60**, 7585 (1999).
10. T. Valla *et al.*, *Phys. Rev. Lett.* **85**, 4759 (2000).
11. R. Corcoran *et al.*, *J. Phys. Condens. Matter* **6**, 4479 (1994).
12. Th. Straub *et al.*, *Phys. Rev. Lett.* **82**, 4504 (1999).
13. W. C. Tonjes, V. A. Greanya, Rong Liu, C. G. Olson, P. Molinié, *Phys. Rev. B* **63**, 235101 (2001).
14. J. E. Graebner, M. Robbins, *Phys. Rev. Lett.* **36**, 422 (1976).
15. Because the sample is in the incommensurate CDW phase at 10 K, one might expect a CDW gap opening. However, we have not been able to measure a clear opening of a gap accompanied by a shift of the leading edge across the CDW transition even at this resolution. One possible reason is the incommensurability of the CDW, because the resistivity does not show an abrupt increase but actually reduces continuously in the incommensurate CDW phase.
16. We have observed the existence of gap anisotropy with a variation of about 20% on the Nb 4d dominant FS sheets, suggesting an anisotropic s-wave gap. We did not observe any anisotropy within the Se 4p dominant band.
17. M. R. Norman, M. Randeria, H. Ding, J. C. Campuzano, *Phys. Rev. B* **57**, R11093 (1998).
18. For the calculations, we fit the spectra in the region from −3.5 to 3.5 meV to estimate the gap value. Ideally, ARPES spectra should show a resolution-limited quasiparticle peak at E_F. Although the width of the peak in the superconducting-state spectra (Fig. 2, B and C) is indeed limited by the resolution, the width in the normal state is very broad, which may be explained in terms of impurity or defect scattering, as was discussed in the ARPES study of 2*H*-$TaSe_2$ (*10*).
19. H. F. Hess, R. B. Robinson, J. V. Waszczak, *Physica B* **169**, 422 (1991).
20. R. Sooryakumar, M. V. Klein, *Phys. Rev. Lett.* **45**, 660 (1980).
21. B. P. Clayman, R. F. Frindt, *Solid State Commun.* **9**, 1881 (1971).
22. M. Nohara, M. Isshiki, F. Sakai, H. Takagi, *J. Phys. Soc. Jpn.* **68**, 1078 (1999).
23. J. A. Sauls, *Adv. Phys.* **43**, 113 (1994).
24. J. Nagamatsu, N. Nakagawa, T. Muranaka, Y. Zenitani, J. Akimitsu, *Nature* **410**, 63 (2001).

25. This work was supported by grants from the Ministry of Education, Culture and Science of Japan. T.K. thanks the Japan Society for the Promotion of Science for financial support.

6 August 2001; accepted 14 November 2001